Measuring and modelling evapotranspiration in a South African grassland: Comparison of two improved Penman-Monteith formulations

Onalenna Gwate[1], Sukhmani K Mantel[1], Anthony R Palmer[1,2]*, Lesley A Gibson[3] and Zahn Munch[4]

[1]*Institute for Water Research, Rhodes University, P.O. Box 94, Grahamstown 6140, South Africa*
[2]*Centre for African Conservation Ecology, Nelson Mandela University, PO Box 77000, Port Elizabeth, 6031, South Africa*
[3]*School of Engineering, University of Edinburgh, EH9 3JL, United Kingdom*
[4]*Department of Geography and Environmental Studies, University of Stellenbosch, P. Bag X1, Matieland, 7602, South Africa*

ABSTRACT

Accurately measuring evapotranspiration (ET) is important in the context of global atmospheric changes and for use with climate models. Direct ET measurement is costly to apply widely and local calibration and validation of ET models developed elsewhere improves confidence in ET derived from such models. This study sought to compare the performance of the Penman-Monteith-Leuning (PML) and Penman-Monteith-Palmer (PMP) ET models, over mesic grasslands in two study sites in South Africa. The study used routine meteorological data from a scientific-grade automatic weather station (AWS) to apply the PML and PMP models. The PML model was calibrated at one site and validated in both sites. On the other hand, the PMP model does not require calibration and hence it was validated in both sites. The models were validated using ET derived from a large aperture scintillometer (LAS). The PML model performed well at both sites with root mean square error (RMSE) within 20% of the mean daily observed ET (R^2 of 0.83 to 0.91). Routine meteorological data were able to reproduce fluxes calculated using micrometeorological techniques and this increased the confidence in the use of data from sparsely distributed AWSs to derive reasonable ET values. The PML model was better able to simulate observed ET compared to the PMP model, since the former models both transpiration and soil evaporation (E_S), while the latter only models transpiration. Hence, the PMP model systematically underestimated ET in a context where the leaf area index (LAI) was < 2.5. Model predictions in the grasslands could be improved by incorporating the E_S component in the PMP model while the PML model could be improved by careful choice of the number of days to be used in the determination of the fraction of E_S.

Keywords: canopy conductance, large aperture scintillometer, model evaluation, parameter estimation, quality control

INTRODUCTION

Evapotranspiration (ET) or its energy equivalent, latent energy flux (*LE*), influences water availability and the partitioning of energy for a given landscape. An understanding of energy and water vapour fluxes over a particular landscape is crucial, especially in a context of validating climate change predictions. This will assist in the use of global change models and also improve the ability to monitor climate change consequences. However, ET is one of the least understood processes of the hydrological cycle, owing to the difficulties inherent in measuring it (Amatya et al., 2016). Recent developments in the form of eddy covariance systems and scintillometers have reduced uncertainties associated with measuring ET. Consequently, many studies have been carried out to evaluate the ability of models in reproducing observed ET (Fisher et al., 2008; Leuning et al., 2008; Mu et al., 2011; Morillas et al., 2013). These studies frequently combine ground-based routine meteorological data and remotely sensed data in developing models.

In the developing world, long-term ET datasets from different vegetation physiognomic types are largely unavailable. In South Africa, the grassland biome comprises 27.9% of the total terrestrial surface of the country and is under pressure from land cover changes related to agriculture and settlement (Mucina et al., 2006). In recent decades the threat from woody invasive alien plants (IAPs) in the grassland biome has been recognised (Kotzé et al., 2010). It is believed that IAPs have a higher ET compared to indigenous species (Meijninger and Jarmain, 2014). Hence, it is critical to identify accurate ET models for grasslands affected by IAPs to improve estimation of ET. Micrometeorological techniques such as scintillometry are costly and this reduces their widespread adoption. At best these micrometeorological methods can be used to calibrate and validate models at a local scale. Most models have been developed elsewhere and have not been locally calibrated or validated, and application of such models remains a challenge due to a paucity of validation datasets. The availability of micrometeorological equipment in data-scarce areas is useful for locally calibrating and validating models to enable widespread applications with higher confidence levels. However, the application of micrometeorological methods is fraught with many challenges owing to the underlying theory and inherent errors (Savage, 2009; Rambikur and Chávez, 2014).

A number of ET models have evolved, ranging from radiation, combination, energy balance and temperature-based algorithms (Mu et al., 2011; Liou and Kar, 2014; Zhang et al., 2016). The Penman-Monteith (PM) equation is one of the most theoretically robust ET models, which is essentially driven by routine meteorological data from weather stations (Fisher et al., 2008; Leuning et al., 2008). The PM equation evolved as a single layer potential ET model (Penman, 1948; Monteith, 1965), but recent efforts have enhanced it to also account for soil evaporation (E_s). One of the recent formulations of the PM equation is the Penman-Monteith-Leuning (PML) equation

* To whom all correspondence should be addressed.
☎ +27466222638;
email: palmert@arc.agric.za
Received 26 September 2017; accepted in revised form 21 June 2018

http://dx.doi.org/10.4314/wsa.v44i3.16
Available on website http://www.wrc.org.za
ISSN 1816-7950 (Online) = Water SA Vol. 44 No. 3 July 2018

(Leuning et al., 2008; Morillas et al., 2013). The biggest challenge in the implementation of the PML model is the determination of canopy conductance (G_c) and the fraction of soil evaporation (f). The f accounts for evaporation from a surface such as bare ground, while G_c influences transpiration. Evaporation from bare soil arguably follows three distinct stages, which include an initial period in which the soil is wet or saturated and ET occurs at or near to a potential rate ($f = 1$). This is followed by a second stage whereby soil is drying and the evaporation rate depends on soil characteristics, which may limit the movement of water into the surface ($f < 1$); and, lastly, dry soil in which the evaporation rate is negligible ($f = 0$) (Hulugalle et al., 2017). Based on this understanding, various algorithms have been developed to simulate soil drying so as to better determine E_s (for example, Leuning et al., 2008; Mu et al., 2011; Morillas et al., 2013; Zhang et al., 2016). Therefore, proper determination of G_c and f is important in order for the model to be able to capture the soil drying process and to adequately account for E_S.

Other recent approaches of the PM equation connect reference ET (ET_0) to actual ET by either using the leaf area index (LAI), vegetation indices (VIs) or crop coefficients (K_c) (Allen et al. 1998; Nagler et al., 2013; Palmer et al. 2014). Due to the robustness of the PM equation and data availability, this study adopted two recent models based on the original PM equation to compare their performance over a grassland area in South Africa. These models include the PML (Leuning et al., 2008; Morillas et al., 2013) and a method described by Palmer et al. (2014), herein called Penman-Monteith-Palmer (PMP). The main difference in the approaches is that the PMP model uses LAI as a scalar while the PML uses G_c and the f to constrain ET. The study used a large aperture scintillometer (LAS) to determine sensible energy flux and then applied the shortened energy balance method to derive *LE*. Subsequently, maximum stomatal conductance of leaves and the rate of soil drying were calibrated. Sensitivity of the PML to wind speed at the canopy was also investigated. The novelty of this study was an assessment of sensitivity of the PML model to components of aerodynamic conductance in short canopies such as grasslands. Finally, the PML and PMP models were validated over grasslands in the Eastern Cape. Validation of the ET models in data-scarce landscapes is important so that wide area ET can be derived in such regions with a higher degree of confidence.

THEORETICAL BACKGROUND

Penman-Monteith-Leuning (PML) model

The PML model advanced the application of the PM equation by translating it into a two-source model (Leuning et al., 2008; Morillas et al., 2013). The PML is expressed as:

$$\lambda E = \frac{\varepsilon A_c + (\rho C_p/\gamma) D_a G_a}{\varepsilon + 1 + \frac{G_a}{G_c}} + f \frac{\varepsilon A_s}{\varepsilon + 1} \quad (1)$$

where the first part represents evaporation from the canopy and the second that from the soil, the terms A_c and A_s (MJ·m^{-2}) are energy fluxes absorbed by the canopy and soil respectively, G_c is canopy conductance (m·s^{-1}), λE is latent energy (MJ·m^{-2}), f is a factor which modulates potential evaporation rate at the soil surface expressed by the equilibrium soil evaporation ($E_{eq,s}$) (Priestley and Taylor, 1972); where $E_{eq,s} = \varepsilon A_s / \varepsilon + 1$), D_a (kPa) is $e_s(T_a) - e_a$, which is the water vapour pressure deficit (VPD) of the air, in which, $e_s(T_a)$ is the saturation water vapour pressure at air temperature and e_a is the actual water vapour pressure, G_a is the aerodynamic conductance (m·s^{-1}), γ is the psychrometric constant (kPa·K^{-1}), ρ is air density (1.2 kg·m^{-3}), C_p is specific heat capacity of air (1 013 J kg^{-1}·K^{-1}), ε is slope (s) of the curve relating saturation water vapour pressure to temperature (kPa K^{-1}) divided by γ, i.e. s/γ.

The procedures described in Allen et al. (1998) were used to derive net radiation while A_s, A_c, G_c and G_a were obtained following Morillas et al. (2013). For daily calculation of ET, ground energy flux (G) was ignored as per the recommendations by Allen et al. (1998).

PMP model

This model uses the leaf area index (LAI) as a proxy for vegetation indices (VIs) or crop coefficients (K_c) to scale reference ET (ET_0) to actual ET (Palmer et al., 2014). The logistics of deriving ET using the PMP model have been described (Palmer and Yunusa, 2011; Weideman, 2013; Palmer et al., 2014). The PMP model is expressed as:

$$ET = \frac{LAI}{LAI_{max}} \times ET_0 \quad (2)$$

where LAI_{max} is the site-specific long-term maximum LAI obtained from MOD15 product (Myneni et al., 2002), ET_0 is short grass reference evapotranspiration calculated using Eq. 6 in Allen et al. (1998).

Large aperture scintillometer (LAS)

A LAS is an instrument that can measure the amount of scattering of electromagnetic radiation caused by turbulence in the atmosphere, through the transmission of a beam of radiation (850 nm) over a horizontal path between a transmitter and a receiver (Kipp and Zonen, 2012). The scintillations are caused by the fluctuations of the refractive index (n) of air along the propagation path and its magnitude can be described by the structure parameter of the refractive index of air (C_n^2), which is the basic parameter derived from scintillometer data (Hill, 1992). The C_n^2 (m$^{-2/3}$) is a representation of atmospheric turbulent strength or the ability of the atmosphere to transport scalars, such as heat, humidity and other atmospheric gases. By applying the Monin-Obukhov Similarity Theory (MOST), surface flux of sensible energy (H) can be determined. For a LAS that has equal apertures, the relationship between the measured variance of the natural logarithm of intensity fluctuations (σ_{lnI}^2) and C_n^2 is as follows (Kipp and Zonen, 2012):

$$C_n^2 = 1.12\, \sigma_{lnI}^2 D^{\frac{7}{3}} L^{-3} \quad (3)$$

where D is the aperture diameter of the LAS, L is the distance between the transmitter and the receiver (i.e. the path length). It should be noted that fluctuations in temperature and humidity also influence C_n^2. Details for the derivation of C_n^2, can be found (for example, (Kohsiek et al., 2002; Meijninger et al., 2002; Kipp and Zonen, 2012). By applying the shortened surface energy balance equation (Savage, 2009), the latent energy flux (*LE*) could be derived if ancillary meteorological data are available:

http://dx.doi.org/10.4314/wsa.v44i3.16
Available on website http://www.wrc.org.za
ISSN 1816-7950 (Online) = Water SA Vol. 44 No. 3 July 2018

$$R_n = H + LE + G, \quad (4)$$

where H, G and R_n are sensible, ground energy flux and net radiation, respectively.

METHODS

Study site

Two experimental sites were selected at Truro and Somerton farms in the northern Eastern Cape (Fig. 1), and micrometeorological measurements were collected using a LAS system. The study sites lie in the grassland biome (Mucina et al., 2006). A field campaign approach was adopted owing to logistical problems (Table 1). Both sites were exposed to moderate grazing by livestock.

Truro site

The first experimental site was at Truro farm. The site was cleared of *Acacia mearnsii* in 2005 and left to re-vegetate naturally. At this site, modelled annual pan evaporation and mean annual rainfall are 1 632 and 786 mm, respectively (Schulze, 1997). Post-clearing, the dominant grass species were *Eragrostis curvula* and *Sporobolus africanus,* with some pockets of *Heteropogon contortus.* Mean canopy height was estimated at 0.15 m after 10 physical measurements at different patches around the path length. Based on the line transect method (Flombaum and Sala, 2007), grass, bare soil, forbs and shrub canopy cover were estimated at 65, 24, 5 and 6%, respectively. The average terrain slope along the path length was 7.4% with a maximum slope of 18.8%. The altitude along the LAS path length ranged from 1 458–1 473 m amsl.

TABLE 1
Characteristics of the study area (DoY = day of year)

Farm name	Lat./long. (Transmitter)	Lat./long. (Receiver)	ET data period	Vegetation type	Elevation (m)
Somerton	31° 9'2.00"S, 28°22'50.00"E	31° 9'2.00"S 28°23'3.00"E	DoY 309, 2015 to DoY 104, 2016	Grassland	1250–1264
Truro	31° 4'10.03"S, 28°17'29.72"E	31° 3'59.08"S 28°17'28.92"E	DoY 265 to 308, 2015	Grassland	1458–1473

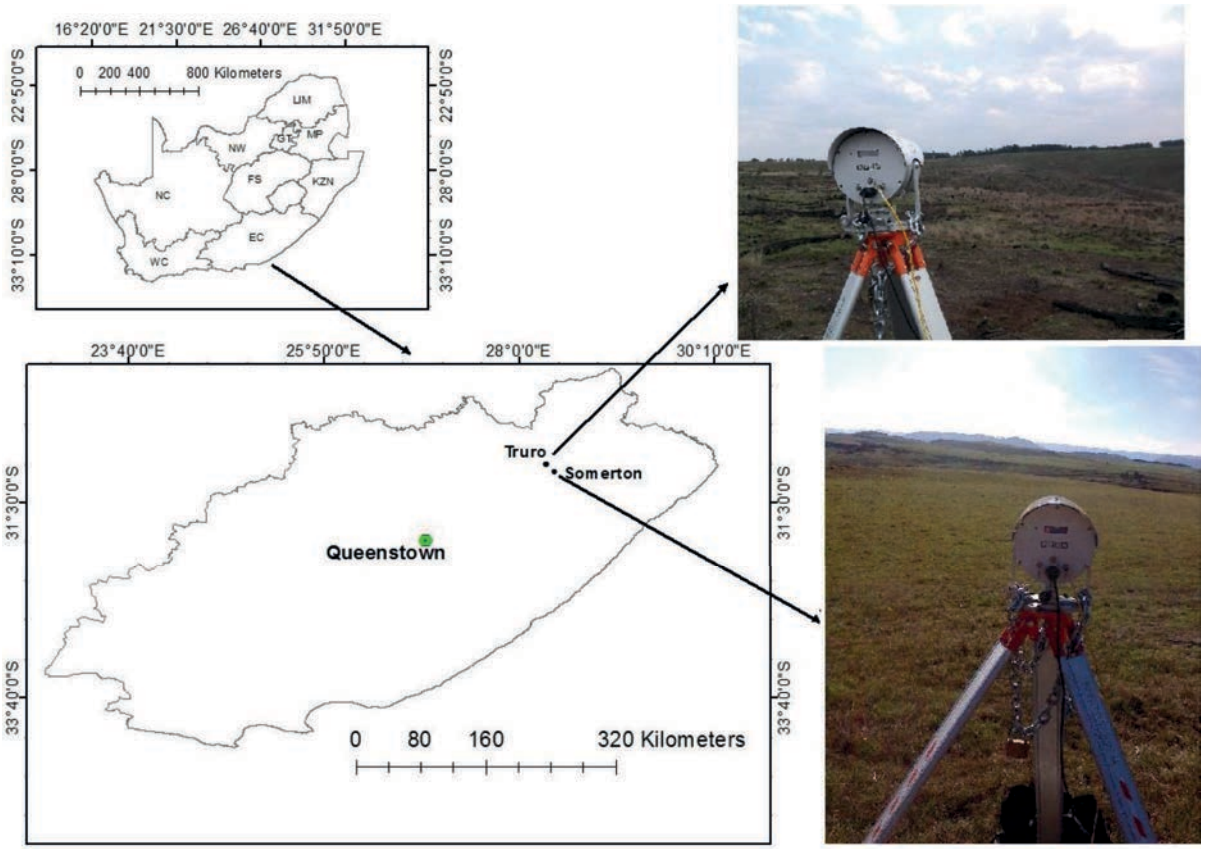

Figure 1
Location of study sites at Truro and Somerton farms

http://dx.doi.org/10.4314/wsa.v44i3.16
Available on website http://www.wrc.org.za
ISSN 1816-7950 (Online) = Water SA Vol. 44 No. 3 July 2018

Somerton site

At the Somerton site, pan evaporation is 1 686 mm per year and long-term mean annual rainfall is approximately 756 mm (Schulze, 1997). The LAS system was installed in a grazing camp and the dominant grass species was *Themeda triandra*. There was no evidence of any other form of historical disturbance (e.g. ploughing) in this camp, and it represented undisturbed native grassland in relatively good condition. At Somerton, the line transect method (Flombaum and Sala, 2007) estimated grass, bare soil, and forb canopy cover at 90, 8 and 2%, respectively. Average canopy height was 0.25 m and altitude ranged from 1 250–1 264 m amsl with an average slope of 0.4% along the LAS path.

Large aperture scintillometer set-up

A large aperture scintillometer (LAS MkII, Kipp and Zonen B.V., Netherlands) was installed firstly at Truro and then at Somerton during the growing season of 2015/2016. This LAS is designed for measuring the path-averaged structure parameter of the C_n^2 over horizontal path lengths from 250 m to 4.5 km and has a 0.149 m diameter (D) beam. The radiation source of the LAS MkII transmitter operates at a near-infrared wavelength of 850 nm. The scintillations measured by the instrument at this wavelength are caused by turbulent temperature fluctuations (Kipp and Zonen, 2012). At Truro farm a suitable patch of relatively homogenous rehabilitated grassland was found with a path length of 458 m, while at Somerton farm the path length was 355 m. Since the path lengths were less than 1 km, 0.1 m aperture diameter restrictors were fitted (Kipp and Zonen, 2012). The instrumental set-up was carefully arranged to ensure that the fetch comprised relatively homogenous grassland vegetation at both study sites. A micro-meteorological station was established at the LAS receiver to measure meteorological variables (Table 2).

The LAS and micro-meteorological station sensors were connected to a Campbell Scientific CR3000 data logger for data recording.

Meteorological data

To determine the utility of sparsely distributed weather stations in modelling ET, independent meteorological data for running the models were obtained from an AWS (Table 3) located 500 m away from the experimental site at Somerton farm and the same weather station data was used to run the PML and PMP models at Truro farm located approximately 14 km away, It should be noted that in South Africa there is a paucity of validation datasets due to the unavailability of ET measurement equipment such as scintillometers on a wide scale. AWSs are more available, albeit sparsely distributed. Therefore, the use of completely independent datasets such as AWS in calibrating and running the ET models could be useful in a context of paucity in validation equipment. However, at the Truro site, the Tropical Applications of Meteorology Using Satellite Data and Ground-Based Observations (TAMSAT) rainfall data for Africa (Maidment et al., 2014; Tarnavsky et al., 2014) were used to drive the PML model, since there was no rainfall station close by. The Mann-Whitney test showed that the TAMSAT data at Somerton farm was similar to the observed rainfall from the AWS at the site (Mann-Whitney U = 3002, $z = -1.08$, $N_1 = N_2 = 85$, $p > 0.05$ two tailed), and subsequently the dataset was applied with a high degree of confidence.

TABLE 2
Bio-meteorological sensors at the Somerton and Truro farm sites

Bio-meteorological variable (hourly)	Instrument
Net radiation ($W \cdot m^{-2}$)	Two net radiometers (NR-lite2) (Delft, Kipp & Zonen, Netherlands)
Temperature (°C) and relative humidity (%)	HC2S3 Temperature and relative humidity Probe (Campbell Scientific Inc., Logan, Utah, USA)
Soil heat flux ($W \cdot m^{-2}$)	4 x soil heat plate (HFP01, Campbell Scientific)
Soil temperature (°C)	2 x averaging soil thermocouples probe (TCAV, Campbell Scientific)
Air temperature (°C)	Fine wire thermocouples (FW05: 0.0005 in /0.0127 mm, Campbell Scientific)
Volumetric soil water content ($m^3 \cdot m^{-3}$)	2 x water content reflectometer (CS616, Campbell Scientific)
Wind speed ($m \cdot s^{-1}$) and direction (degrees)	Wind Monitor-AQ, model 05305 (R.M. Young Company, Michigan, USA)
Air pressure (kPa)	CS106 Barometric pressure sensor (Campbell Scientific)

TABLE 3
Meteorological data measured at the Agricultural Research Council's automatic weather station and instrumentation at Somerton farm

Weather parameter (daily)	Instrument
Solar radiation ($MJ \cdot m^{-2}$)	Pyranometer (LI-200SA)
RH (%) and air temperature (°C)	Vaisala HMP60 Temp/humidity probe (HMP60)
Wind speed ($m \cdot s^{-1}$) and direction (degrees)	R.M. Young wind sentry wind set (Model 03001)
Rainfall (mm)	Texas Electronics Rain Gauge 0.1 mm (0.00394 in, TE525 mm-L)

http://dx.doi.org/10.4314/wsa.v44i3.16
Available on website http://www.wrc.org.za
ISSN 1816-7950 (Online) = Water SA Vol. 44 No. 3 July 2018

Wind speed estimation

The PML is sensitive to the aerodynamic components when applied in short canopies and wind speed was estimated at the canopy height instead of using wind speed measured at the reference height of 2 m (Allen et al., 1998). The study applied a power law equation described by Manwell et al. (2002) in extrapolating wind speed to different heights. The equation applied is as follows:

$$V_x = V_2\left(\frac{h_x}{h_2}\right)^{\grave{a}} \quad (5)$$

where V_x is the wind speed at the height to be extrapolated i.e. h_x canopy height), V_2 is the wind speed recorded by the agro-meteorological stations at 2 m from the ground level i.e. h_2 = 2 m, and the power law exponent (à) is the wind shear exponent (Manwell et al., 2002). The à was calculated as follows:

$$\grave{a} = (0.37 - 0.0881 \ln V_2)/[1 - 0.0881 \ln (h_2/h_x)] \quad (6)$$

Determining the fraction of soil evaporation (f) and maximum stomatal conductance (g_{sx})

Three methods for determining f were applied. These included the f_{Zhang} (Zhang et al., 2010), f_{drying} and measured volumetric soil water content (f_{SWC}) (Morillas et al., 2013). In order to successfully apply the f_{drying} approach, the CLIMWAT database (FAO, 2013) was used to determine daily effective precipitation, which was estimated at 1.65 mm for the study site. To successfully implement the f_{SWC} approach, the minimum volumetric soil water content (θ_{min}), was obtained from another study site at eZulu Game Reserve (Gwate et al., 2016), which had a longer soil moisture record including the driest months. This was assumed to be representative since the two sites have similar geology, namely Beaufort Series sandsones of the Karoo Supergroup (Mucina et al., 2006).

Moderate imaging spectroradiometer (MODIS) data

The study used the LAI derived from MOD15A2 FPAR/LAI product (Myneni et al., 2002) to drive the PML model. Surface albedo was obtained from the MCD43B4 (Strahler and Muller, 1999) product by applying Liang's (2001) equation.

Data analysis

The accuracy of the energy fluxes from a LAS is influenced by the mean height of its optical beam above the surface. EVATION (evapotranspiration) software program v2.5.0.11 (Kipp and Zonen B.V.) was used to determine effective LAS beam height following Hartogensis et al. (2003). A slope profile along the path length was generated using elevation data from Google EarthPro and EVATION to derive effective height. A number of parameters in EVATION were configured before analysis could be carried out. These included selection of LAS Mk11, the momentum roughness length (z_{om}) and the displacement height (d). Vegetation height was estimated at different locations and times during the experiment in order to derive mean canopy height by measuring representative patches, with z_{om} and d determined from the estimated canopy height (h) as 0.1 h and 0.66 h, respectively (Allen et al., 1998). Data were downloaded from the LAS and analysed using EVATION. The derived LE values were then converted into mm·h^{-1} to obtain ET.

Data quality control

During processing, LAS data were controlled using several quality checks (QC). Data were filtered for low signal (demodulated signal less than 10 mV as per requirements of EVATION software). Poor quality data were removed after the misalignment between the LAS transmitter and receiver. The Bowen ratio (β) was also used to reject positive fluxes when β > 3, since H would be far larger than LE and the latter insignificant. Any data points where the β was between −0.05 and 0 were removed, due to instability of the solution for this extreme value range (Rambikur and Chávez, 2014). Data during precipitation events were also excluded. Positive fluxes during periods between 05:00 and 06:00 with friction velocity (u_*) less than 0.1 m·s^{-1} were also filtered out to avoid conditions with poorly developed turbulence. Periods with a temperature difference of less than 0.2°C between the lower and upper air temperature sensors were filtered out to avoid the risk of inaccurate determination of atmospheric stability. The upper scintillation saturation criterion was also considered as a potential basis for rejecting fluxes based on:

$$C_n^2 < 0.057\, D^{5/3} L^{-8/3}\, \lambda^{1/3} \quad (7)$$

where D is the beam diameter (m), L is the pathlength (m) and λ is the scintillometer optical wavelength (nm) (Kohsiek et al., 2002; Bouin et al., 2012).

Calibration of the PML model

Average hourly latent energy flux (LE) estimates were converted to actual ET (mm·h^{-1}) and summed into daily totals before being used in this study. The PML model requires the calibration of the maximum stomatal conductance (m·s^{-1}) of leaves at the top of the canopy (g_{sx}) and the rate of soil drying (α, day^{-1}). The calibration period spanned from DoY 308 to 359, 2015. Despite the short period, varied environmental conditions that represent both growing and non-growing seasons were captured. The g_{sx} and α model parameters were estimated by optimisation using the 'rgenoud' package (Mebane and Sekhon, 2011) in R statistical software (Version 3.1.3). The parameter estimation exercise sought to find the values of g_{sx} and α that minimised the cost function (F) over the optimization period (N):

$$F = \frac{\sum_{i=1}^{N} \left| E_{est,i} - E_{obs,i} \right|}{N} \quad (8)$$

where $E_{est,i}$ is the modelled ET for day i, $E_{obs,i}$ is observed ET for day i and N are the number of sample days.

It should be noted that due to logistical challenges, which did not allow for a long time period of measurements at the Truro site, the PML model was validated using g_{sx} and α values obtained from the Somerton site. The two sites are 14 km apart and have similar soils and vegetation type (Mucina et al., 2006).

Stomatal conductance measurements

At the Somerton site, a leaf porometer (Decagon Devices, US/Canada) was used to measure stomatal conductance at a leaf scale and this assisted in comparing measured and optimised stomatal conductance values. The measurements were conducted

http://dx.doi.org/10.4314/wsa.v44i3.16
Available on website http://www.wrc.org.za
ISSN 1816-7950 (Online) = Water SA Vol. 44 No. 3 July 2018

on a week-long field campaign in the morning (08:00–10:00), midday (12:00–14:00) and late afternoon (15:00–16:30).

Model evaluation

The PML and PMP models were then evaluated using the measured LAS ET data. The validation period spanned from DoY 21 to 104, 2016, for both models. Model performance was evaluated using the root mean square error (RMSE) and both the systematic and unsystematic (Willmott, 1981) components are reported. The study also reports the RMSE-observations standard deviation ratio (RSR), which gives a measure of what is considered a low RMSE (Moriasi et al., 2007). The mean absolute error (MAE), which is less sensitive to extreme values than RMSE, is also reported as well as the per cent bias (PBIAS), to give insights into the tendency of models to over- or underestimate the fluxes. The linear regression between the observed and modelled ET was also assessed. Model II simple linear regression using the standard major axis (SMA) method in R statistical software environment (R-3.1.3) was performed. This was found suitable for the study since the two variables of interest were amenable to measurement error (Legendre, 2013). The coefficient of determination (R^2) the slope and y-intercepts were also investigated and reported.

Sensitivity analysis

The sensitivity of the PML to the aerodynamic components was assessed using a complete year (2012) of data over the grassland at Cala, near the present study sites. This was achieved by varying the canopy height, height of wind speed measurement and by extrapolating wind speed measured at 2 m down to the canopy height by applying Eq. 5. Differences in the estimated ET were then recorded for comparison purposes.

RESULTS

Data availability

The effective scintillometer beam height (Z_{LAS}) at Truro was 3.83 m while at Somerton it was 3.05 m (Fig. 2). A total of 39% of the data at Somerton farm was lost, mainly due to misalignment of the unit resulting in no or lower signal strength (Udemond < 10 mV) and a lower C_n^2 of 10^{-17} ($m^{-2/3}$) or no number. With respect to Truro farm, 29% of the data were rejected due to misalignment of the system. The misalignment was mainly caused by animals, which occasionally interfered with the system. Of the available data, 7% and 35% of hourly fluxes were filtered out due to failure to pass quality control

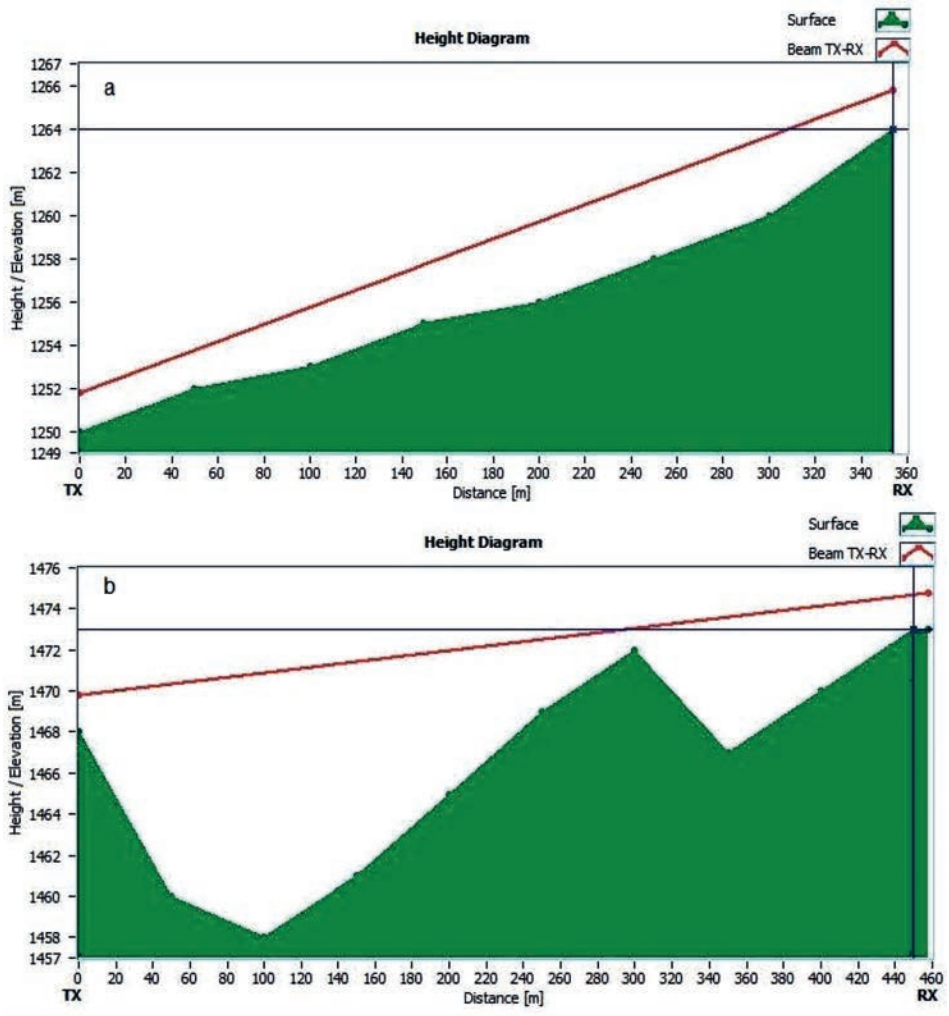

Figure 2
Path length beam and underlying surface topography between the LAS transmitter (TX) and receiver (RX) at (a) Somerton and (b) Truro farms

http://dx.doi.org/10.4314/wsa.v44i3.16
Available on website http://www.wrc.org.za
ISSN 1816-7950 (Online) = Water SA Vol. 44 No. 3 July 2018

flags in Truro and Somerton sites, respectively. Based on Eq. 7, LAS saturation would start at $C_n^2 > 1.85498 \times 10^{-9}$ and 9.3334×10^{-10} at the Truro and Somerton sites, respectively. However, the study did not detect any saturation at either of the sites.

Daily meteorological conditions

Meteorological conditions differed at the study sites (Table 4). With respect to the Somerton site, the prevailing wind was from between the ENE and E sector (24%, Fig. 3a). At the Truro site, the prevailing winds were from the SE and NE direction (Fig. 3b).

At both sites, the ET pattern followed that of SWC and ET_0 was consistently higher than actual ET (Fig. 4).

TABLE 4
Daily meteorological conditions during the calibration period at Somerton farm and validation at Truro farm (mean ± standard deviation)

Variable	Somerton (*N* = 67 days)	Truro (*N* = 29 days)
Mean air temperature (°C)	19.5 ± 3	18.2 ± 2.5
Mean RH (%)	49.1 ± 27	58.2 ± 16.3
Net radiation ($MJ \cdot m^{-2}$)	12 ± 4.8	8.6 ± 3.0
Wind speed ($m \cdot s^{-1}$)	2.74 ± 0.6	3.3 ± 0.8
ET_0 (mm)	4.8 ± 1.7	4.8 ± 1.3
Actual ET (mm)	3.5 ± 1.3	2.23 ± 1.1
Rainfall	1.3 ± 2.3	1.65 ± 3.1
LAI ($m^2 \cdot m^{-2}$)	1.1	0.78 ± 0.1
Volumetric soil water content (SWC $m^3 \cdot m^{-3}$)	0.09 ± 0.2	0.14 ± 0.2

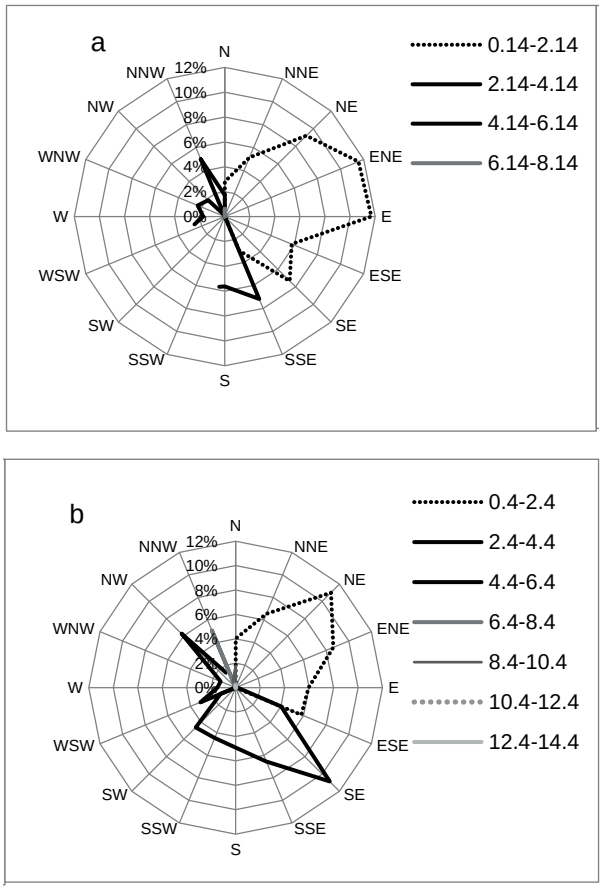

Figure 3
Wind speed ($m \cdot s^{-1}$) and wind direction at (a) Somerton farm and (b) Truro farm during the field campaign

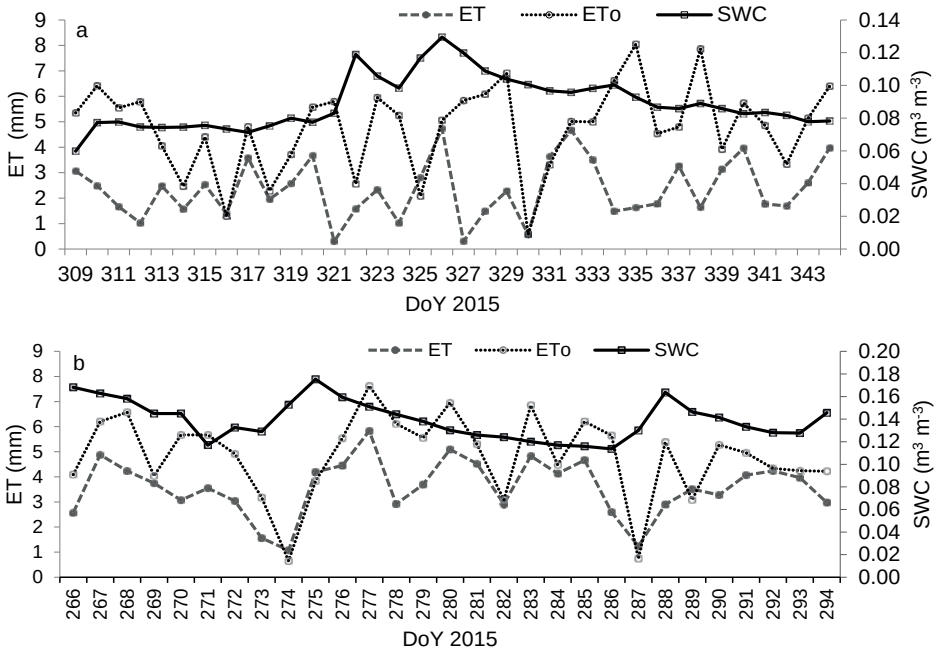

Figure 4
Trends in volumetric soil water content (SWC), reference evapotranspiration (ET_0) and scintillometer evapotranspiration (ET): (a) Somerton and (b) Truro farms

http://dx.doi.org/10.4314/wsa.v44i3.16
Available on website http://www.wrc.org.za
ISSN 1816-7950 (Online) = Water SA Vol. 44 No. 3 July 2018

PML model parameter estimation at Somerton farm

The optimised g_{sx} was similar for the different parameterisation approaches of the PML model and the α was relatively low (Table 5). The measured highest stomatal conductance at the leaf level was 0.0025 m·s^{-1}.

Validation of the PML and PMP models at Somerton farm

All the PML approaches yielded RMSE that was within 15% of the daily observed ET at Somerton farm (Table 6). The average observed ET during validation was (3.5 ± 1.3) mm·day^{-1}. The f_{drying} approach yielded a better model fit while the f_{Zhang} performed poorly compared to the other approaches of the PML (Table 6). The f_{drying} and f_{Zhang} approaches tended to overestimate the observed ET. However, the f_{SWC} approach and the PMP model tended to underestimate the measured ET, as shown by the PBIAS (Table 6). The PMP model had a RMSE of 1.76 mm·day^{-1} and PBIAS of 67%. Most of the RMSE was unsystematic for the two models (Table 6). The MAE for the PML lay between 5 and 10% of the observed daily mean ET while that of the PMP model was 50% of the observed mean ET (Table 6).

TABLE 5
Optimized values for PML model parameters

Approach	g_{sx} (m·s^{-1})	α (day^{-1})
f_{drying}	0.002	0.10
f_{Zhang}	0.0025	N/A
f_{SWC}	0.0023	N/A
Parameter ranges	0.002–0.02	0–1

Validation of the PML and PMP models at Truro farm

The lowest RMSE was obtained with the f_{SWC} approach and the highest with f_{drying} (Table 6). The PMP and the PML model's f_{drying} approach tended to underestimate observed ET (Table 7). With respect to the PMP model and the f_{SWC} approach, the RMSE was essentially systematic, while it was unsystematic for the f_{drying} and f_{Zhang} approaches (Table 7). The average measured daily ET during the validation period was (2.2 ± 0.9) mm and the RMSE for the PML approaches was within 20% of the observed daily ET (Table 7).

Variation in ET

The PML model tended to overestimate ET after rainfall events (Fig. 5). The SWC followed the rainfall pattern at both sites (Fig. 5).

Data from the two sites were combined and regression equations of the modelled ET against observed ET were developed for each site by summing up 8-day ET (N = 15, 8-day periods) in line with the availability of the MODIS LAI. Large regression slopes were obtained using the f_{drying} and f_{Zhang} approaches (Fig. 6a-b). The f_{Zhang} and the f_{SWC} approaches had similar R^2 although their slopes were different (Fig. 6b-c). The lowest R^2 and slope were observed from the PMP model (Fig. 6d).

Sensitivity analysis

Canopy height, wind speed and height of wind speed measurement help to define G_a. It was shown that variation in these G_a components has serious consequences to the PML modelled ET (Table 8).

TABLE 6
Models performance at Somerton farm (, f_{Zhang} and f_{SWC} are the different approaches of the PML model)

Statistics	f_{drying}	f_{Zhang}	f_{SWC}	PMP model
MAE (mm)	0.18	0.37	0.34	1.76
RMSE (mm)	0.26	0.48	0.4	1.89
RSR	0.26	0.06	0.41	1.94
PBIAS (%)	−0.63	−4.1	3.33	67
Systematic RMSE (%)	3	20	7.8	33
Unsystematic (%)	9	44	13	74
Daily modelled mean ET (mm)	3.6 ± 1.37	3.74 ± 1.59	3.44 ± 1.1	1.7 ± 0.86

TABLE 7
Models performance at Truro farm (f_{drying}, f_{Zhang} and f_{SWC} are the different approaches of the PML model)

Statistics	f_{drying}	f_{Zhang}	f_{SWC}	PMP model
MAE	0.21	0.26	0.25	1.38
RMSE	0.41	0.34	0.30	1.45
RSR	0.52	0.77	0.7	3.34
PBIAS	4.2	-1.2	-0.36	68.7
Systematic RMSE (%)	8.4	8	13.4	72
Unsystematic (%)	17	15	10	35
Daily modelled mean ET (mm)	2.1 ± 0.6	2.2 ± 0.66	2.2 ± 0.63	1.31 ± 0.5

http://dx.doi.org/10.4314/wsa.v44i3.16
Available on website http://www.wrc.org.za
ISSN 1816-7950 (Online) = Water SA Vol. 44 No. 3 July 2018

TABLE 8
Model sensitivity to aerodynamic components at Cala (January–December 2012)

Canopy height (m)	Height of wind speed measurement (m)	Total ET (mm)
0.12	2	1 158.7
0.5	2	1 025.6
0.5*	2	572.3
0.5**	0.5	451.7

**wind speed at 2 m was extrapolated to wind speed at 0.5 m (canopy height) using the power law and height of wind measurement was maintained at 2 m.*
***wind speed at 2 m was extrapolated to wind speed at 0.5 m (using the power law) and canopy height (0.5 m) was used.*

DISCUSSION

Data quality

Good quality data are crucial for model calibration and validation. The study applied well-established and rigorous data quality control protocols in order to accurately derive fluxes (Campbell Scientific, 2005; Bouin et al., 2012; Rambikur and Chávez, 2014) and this helped to reduce uncertainties in the calculated ET. The good performance of the PML model on the Truro farm, where only validation was done using calibrated values of α and g_{sx} from the Somerton site, suggests that the obtained values could be accurate given that environmental conditions also differed during the calibration and validation periods. Although there were isolated high pulses of ET,

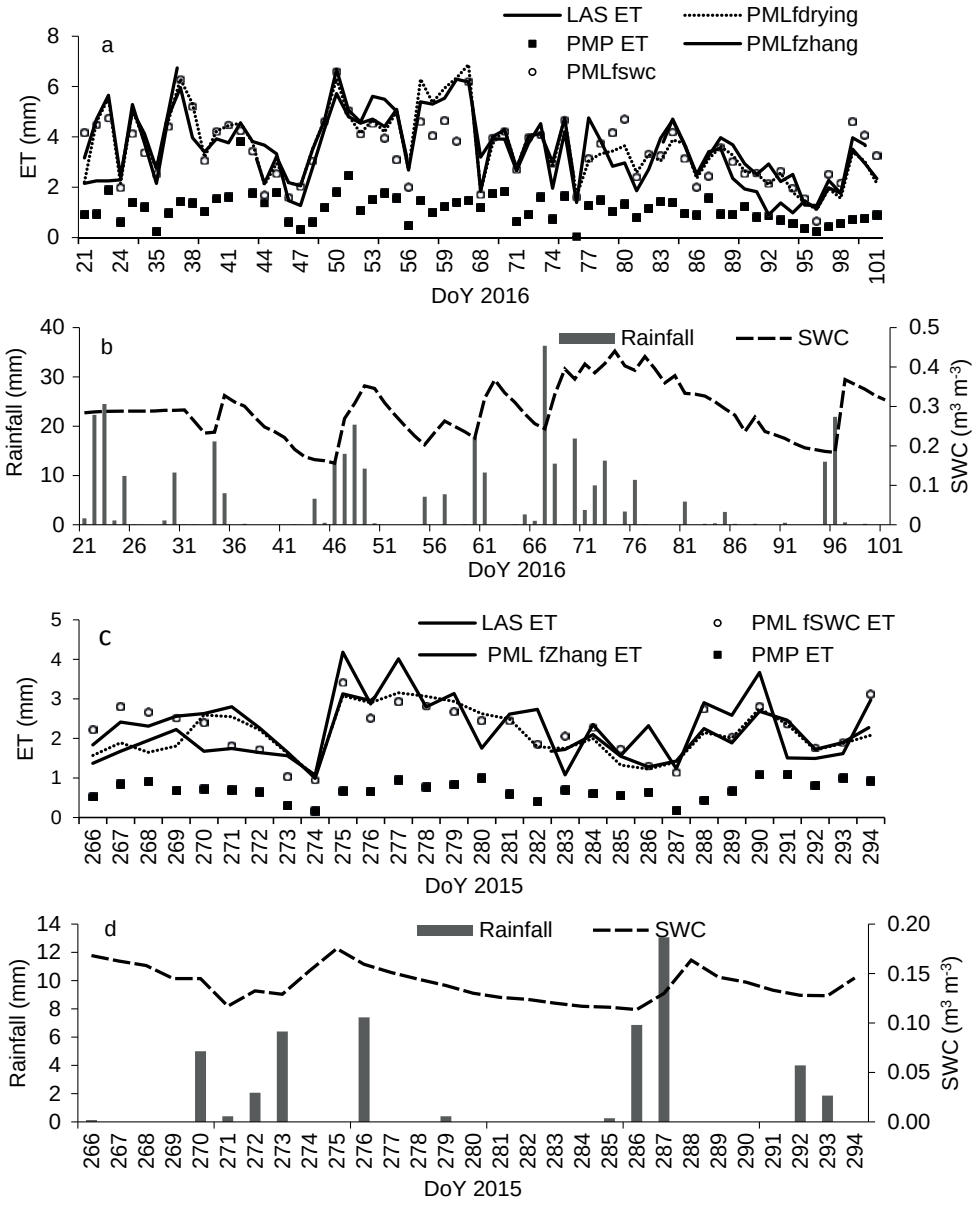

Figure 5
Daily variation in measured evapotranspiration (LAS ET) and modelled ET: (a) Somerton farm (PML f_{drying}, PML f_{drying}, PML f_{SWC} and PMP ET models), (b) Daily variation in rainfall and volumetric soil water content (SWC) at Somerton farm, (c) Daily variation in measured evapotranspiration (LAS ET) and modelled ET at Truro farm (PML f_{drying}, PML f_{Zhang}, PML f_{SWC} and PMP ET models) and (d) Daily variation in rainfall and volumetric soil water content (SWC) at Truro farm.

http://dx.doi.org/10.4314/wsa.v44i3.16
Available on website http://www.wrc.org.za
ISSN 1816-7950 (Online) = Water SA Vol. 44 No. 3 July 2018

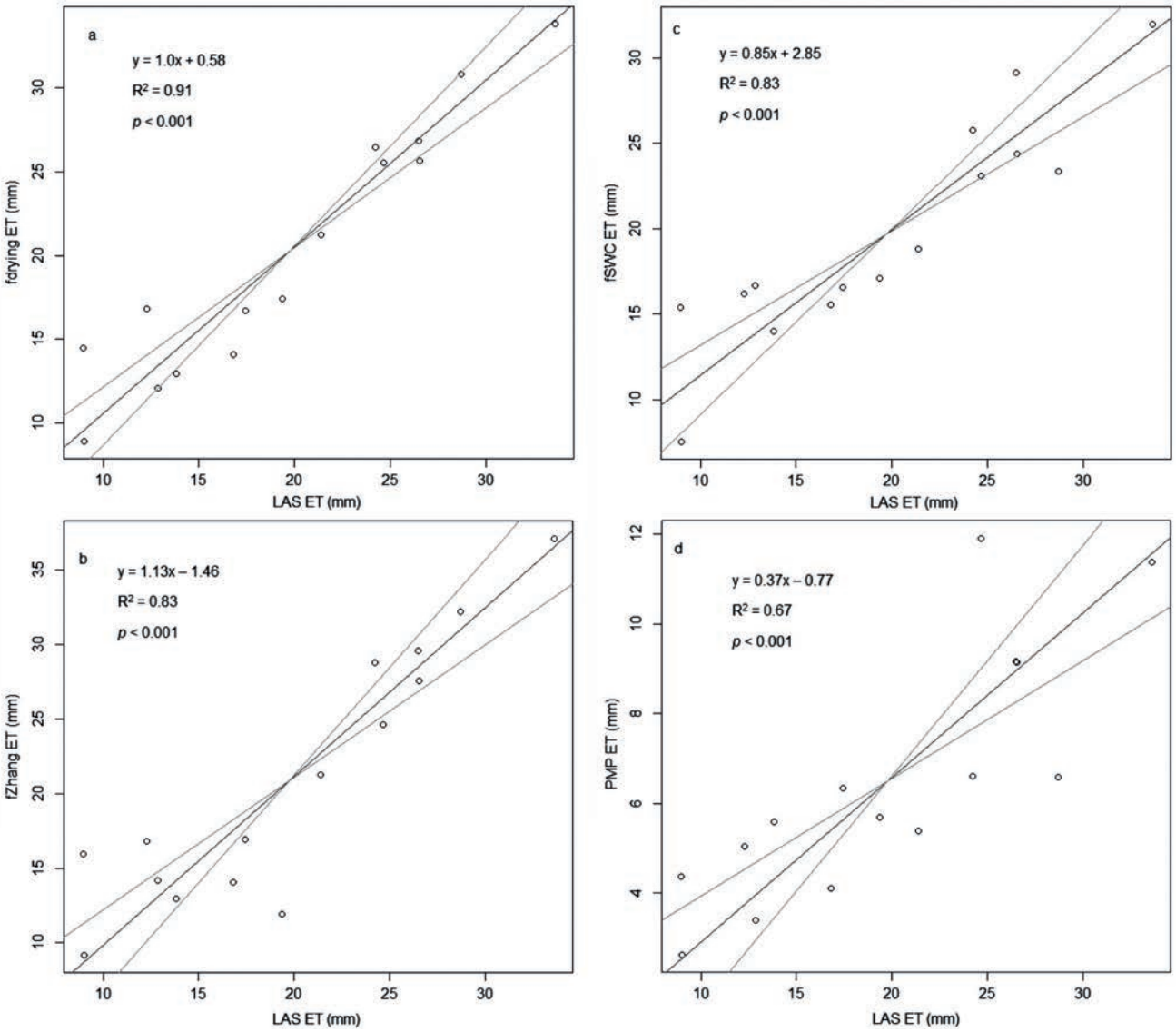

Figure 6

Relationship between observed and modelled ET for the two study sites (combined data) with 95% confidence limits

generally the atmospheric demand for moisture was high at the sites as ET was less than ET_0 for most of the time, suggesting that the areas were water limited.

Calibrated model parameters

The estimated values of g_{sx} were similar for the three approaches for parameterising conductance, indicating convergence in the methods. The g_{sx} values were slightly lower than the optimised values obtained by Leuning et al. (2008) in Kendall, USA, who obtained a value of 0.0048 $m \cdot s^{-1}$ over a grassland, but the observed values were within the limits reported by Kelliher et al. (1995). The highest measured stomatal conductance value obtained was 0.0025 $m \cdot s^{-1}$. It is well established that the dominant species at Somerton (*Themeda trianda*) and at Truro farm (*E. curvula*) have evolved to survive in semi-arid areas by reducing stomatal conductance in order to optimise water use (Snyman et al., 2013; Favaretto et al., 2015). In addition, C4 grasses similar to those at the study sites have relatively small stomata, regardless of density, resulting in a lower maximum stomatal conductance to water vapour (Liu and Osborne, 2014). Hence, a combination of these factors and the size of the crop (0.15–0.25 m) could explain the relatively low optimised g_{sx}. The α was low (0.1) and this may be reflective of relatively high SWC.

Performance of the PML model

The f_{drying} approach outperformed the other PML approaches and the PMP model in reproducing ET dynamics. However, the slight over-prediction by the f_{drying} approach was due to the higher f values considered by the model, probably due to relatively high precipitation during the validation period at the Somerton site. There were only a few rainy days during validation at Truro, resulting in lower f values and hence the slight underestimation by the model at this site. This is also true with respect to the f_{Zhang} approach, although it still overestimated ET at the Truro farm site. This was consistent with Morillas et al. (2013) who also observed that, when applied on a daily interval, the f_{Zhang} approach tended to over-predict ET, especially after rainfall events. Zhang et al. (2016) also reported slight overestimation

http://dx.doi.org/10.4314/wsa.v44i3.16
Available on website http://www.wrc.org.za
ISSN 1816-7950 (Online) = Water SA Vol. 44 No. 3 July 2018

of ET by the f_{Zhang} PML approach. The performance of the f_{Zhang} approach suggests that it is a robust method and could reduce the number of parameters needed in the PML model. The slight underestimation of ET by the f_{SWC} at Somerton farm could be linked to errors associated with rescaling volumetric soil water content to f values. With respect to the three approaches of the PML, most of the RMSE was unsystematic and this is a hallmark of robust models (Willmott 1981; Leuning et al. 2008). Overall, the RMSE and MAE for the different PML approaches were significantly lower, relative to mean daily measured ET, and this suggests that the model was quite robust. Morillas et al. (2013) found R^2 of 0.24–0.59 using different approaches of the PML while this study obtained higher R^2 results. Although α was kept constant, reasonably good results were still obtained. It should be noted that in reality α is dynamic since it is influenced by changing environmental conditions (Morillas et al., 2013).

Performance of the PMP model

The poor performance by the PMP model shows that scaling ET_0 to actual ET through MODIS LAI may not be adequate in areas with low LAI. It is well established that at low LAI (< 2.5), E_s could be as high as 80% of the total flux (Morillas et al., 2013). In addition, short canopies may not be effective in attenuating energy through the canopy to the soil surface and this could have resulted in high A_s to drive E_s. The LAI in the study area was < 2 and as such the PMP model could not capture the dynamics in ET. Hence, the model systematically underestimated ET owing to the low scaling factor. It should be noted that the MODIS LAI product is only provided every 8 days yet the grassland responds very rapidly to rain events, and the delay in acquiring the latest LAI after the first rain events would have meant that, in the first days of validation, model predictions were compromised. Given that the PMP is a parsimonious model forced by readily available data, it is prudent to incorporate E_s in the formulation in order to improve ET estimation. However, Palmer et al. (2014) found a good model fit using the PMP model in a semi-arid savanna of South Africa; hence, vegetation physiognomic structure could explain the disparity in results.

Sensitivity analysis of the PML model

When applying the PML it is important to accurately determine aerodynamic components as shown by sensitivity analysis of the model over the grassland. Results suggest that over short canopies, ET can easily be over-estimated if wind speed at the reference height is used. High wind speed was recorded at the reference height of 2 m compared to the actual wind speed at the canopy. The increase in the height of wind speed measurement, results in an increase in the modelled ET. Hence, in areas characterised by short vegetation such as grassland, the estimation of the wind speed at the canopy height is crucial in order to derive accurate fluxes.

CONCLUSIONS

The study compared the performance of the PML and PMP models against ET derived from a LAS over grasslands. Based on the model evaluation metrics, the PML performed better than the PMP model. Hence, the calibrated values may be applied across grasslands in South Africa with reasonable confidence. The good performance by the f_{Zhang} approach was encouraging since the PML can now be applied using data that is readily available, with only g_{sx} as a model parameter to be determined. Routine meteorological data were able to reproduce fluxes calculated using micrometeorological methods over this grassland. This means sparsely distributed weather stations can confidently be used to derive reasonable ET over wide areas, as the validation exercise revealed. Determining accurate wind speed at the canopy height is crucial when working in short vegetation in order to derive reasonable ET estimates using the PML model. The inadequacy of the PMP model to simulate observed ET in the study area confirmed the importance of E_s in such environments and, therefore, the PMP model could be improved by adding a E_s component.

ACKNOWLEDGEMENTS

This work was supported by the South African Water Research Commission, as part of Project No. K5/2400/4, and the National Research Foundation through the National Equipment Fund. Special thanks go to the Du Pleis and Trollop families who allowed the project team to install equipment on their properties.

REFERENCES

ALLEN R G, PEREIRA LS, RAES D and SMITH M (1998) Crop evapotranspiration (guidelines for computing crop water requirements). FAO Irrigation and Drainage Paper No. 56. Food and Agricultural Organization of the United Nations, Rome.

AMATYA DM, IRMAK S, GOWDA P, SUN G, NETTLES JE and DOUGLAS-MANKIN KR (2016) Ecosystem evapotranspiration: challenges in measurements, estimates, and modeling. *Trans. ASABE* **59** (2) 555–560. https://doi.org/10.13031/trans.59.11808

BOUIN MN, LEGAIN D, TRAULLE Q, BELAMARI S, CANIAUX G, FIIANDRINO A, LAGARDE F, BARRIE J, MOULIN E and BOUHOURS G (2012) Using scintillometry to estimate sensible heat fluxes over water: first insights. *Boundary-Layer Meteorol.* **143** 451–480. https://doi.org/10.1007/s10546-012-9707-8

CAMPBELL SCIENTIFIC (2005) Bowen ratio instrumentation revision: 9/05. Instruction Manual. Campbell Scientific Inc. URL: https://s.campbellsci.com/documents/au/manuals/bowen.pdf. (Accessed 16 October 2016).

FAO (2013) CLIMWAT 2.0 for CROPWAT. URL: http://www.fao.org/nr/water/infores_databases_climwat.html (Accessed 16 August 2016)

FAVARETTO A, SANTOS J, CARNEIRO CM and BASSO SMS (2015) The first anatomical and histochemical study of tough lovegrass (*Eragrostis plana* Nees, Poaceae). *Afr. J. Agric. Res.* **10** (30) 2940–2947. https://doi.org/10.5897/AJAR2014.9145

FISHER JB, TU KP and BALDOCCHI DD (2008) Global estimates of the land-atmosphere water flux based on monthly AVHRR and ISLSCP-II data, validated at 16 FLUXNET sites. *Remote Sens. Environ.* **112** (3) 901–919. https://doi.org/10.1016/j.rse.2007.06.025

FLOMBAUM P and SALA O E (2007) A non-destructive and rapid method to estimate biomass and aboveground net primary production in arid environments. *J. Arid Environ.* **69** (2) 352–358. https://doi.org/10.1016/j.jaridenv.2006.09.008

GWATE O, MANTEL SK, PALMER AR and GIBSON AL (2016) Measuring evapotranspiration using an eddy covariance system over a subtropical thicket of the Eastern Cape, South Africa. In: *SPIE Remote Sensing for Agriculture, Ecosystems, and Hydrology XVIII* (Vol. 9998, p. 99980S), 26–29 Sepember, Edinburgh.

HARTOGENSIS OK, WATTS CJ, RODRIGUEZ J-C and DE BRUIN HAR (2003) Derivation of an effective height for scintillometers: La Poza experiment in Northwest Mexico. *Hydrometeorol.* **4** (5) 915–928. https://doi.org/10.1175/1525-7541(2003)004<0915:DOAEHF>2.0.CO;2

HILL RJ (1992) Review of optical scintillation methods of measuring the refractive-index spectrum, inner scale and surface fluxes. *Waves Random Media* **2** (3) 179–201. https://doi.org/10.1088/0959-7174/2/3/001

HULUGALLE NR, WEAVER TB and FINLAY LA (2017) Fallow soil evaporation in a grey Vertisol under contrasting wheat stubble

management practices in cotton cropping systems. *Soil Tillage Res.* **165** 41–45. https://doi.org/10.1016/j.still.2016.07.011
KELLIHER FM, LEUNING R, RAUPACH MR and SCHULZE ED (1995) Maximum conductances for evaporation from global vegetation types. *Agric. For. Meteorol.* **73** (1–2) 1–16. https://doi.org/10.1016/0168-1923(94)02178-M
KIPP and ZONEN (2012) Instruction Manual: LAS MkII Scintillometer. URL: www.kippzonen.com/Download/101/LAS-MkII-ET-system-Manual (Accessed 20 April 2016)
KOHSIEK W, MEIJNINGER WM, MOENE AF, HEUSINKVELD BG, HARTOGENSIS OK, HILLEN WCAM and DE BRUIN HAR (2002) An extra large aperture scintillometer for long range applications. *Boundary-Layer Meteorol.* **105** (1) 119–127. https://doi.org/10.1023/A:1019600908144
KOTZÉ I, BEUKES H, VAN DEN BERG E and NEWBY T (2010) National invasive alien plant survey. Report No. GW/A/2010/21. Agricultural Research Council, Institute for Soil, Climate and Water, Pretoria. URL: http://wis.orasecom.org/content/study/Data (Accessed 16 April 2016).
LEGENDRE P (2013) Model II regression user's guide, R edition. *R Vignette* **4** 1–14. URL: http://ftp-nyc.osuosl.org/pub/cran/web/packages/lmodel2/vignettes/mod2user.pdf (Accessed 23 March 2016).
LEUNING R, ZHANG YQ, RAJAUD A, CLEUGH HA and TU K (2008) A simple surface conductance model to estimate regional evaporation using MODIS leaf area index and the Penman-Monteith equation. *Water Resour. Res.* **45** (W10419). https://doi.org/10.1029/2007WR006562
LIANG S (2001) Narrowband to broadband conversions of land surface albedo I Algorithms. *Remote Sens. Environ.* **76** 213–238. https://doi.org/10.1016/S0034-4257(00)00205-4
LIOU Y-A and KAR S (2014) Evapotranspiration estimation with remote sensing and various surface energy balance algorithms—a review. *Energies* **7** (5) 2821–2849. https://doi.org/10.3390/en7052821
LIU H and OSBORNE CP (2014) Water relations traits of C4 grasses depend on phylogenetic lineage, photosynthetic pathway, and habitat water availability. *J. Exp. Bot.* **66** (3) 761–773. https://doi.org/10.1093/jxb/eru430
MAIDMENT RI, GRIMES D, ALLAN PR, TARNAVSKY E, STRINGER M, HEWISON T, ROEBELING R and BLACK E (2014) The 30 year TAMSAT African Rainfall Climatology And Time series (TARCAT) data set. *J. Geophys. Res. Atmos.* **119** 10619–10644. https://doi.org/10.1002/2014JD021927
MANWELL JF, MCGOWAN JG and ROGERS AL (2002) Wind energy explained: theory, design and application. John Wiley & Sons, West Sussex.
MEBANE WRJ and SEKHON J S (2011) Genetic optimization using derivatives: the rgenoud package for R. *J. Stat. Softw.* **42** (11) 1–26.
MEIJNINGER WML and JARMAIN C (2014) Satellite-based annual evaporation estimates of invasive alien plant species and native vegetation in South Africa. *Water SA* **40** 95–108. https://doi.org/10.4314/wsa.v40i1.12
MEIJNINGER WML, HARTOGENSIS OK, KOHSIEK W, ZUURBIER RM and DE BRUIN HAR (2002) Determination of area-averaged sensible heat fluxes with a large aperture scintillometer over a heterogeneous surface – Flevoland field experiment. *Boundary-Layer Meteorol.* **105** 37–62. https://doi.org/10.1023/A:1019647732027
MONTEITH JL (1965) Evaporation and environment. *Symp. Soc. Exp. Biol.* **19** 205–234.
MORIASI DN, ARNOLD JG, VAN LIEW MW, BINGER RL, HARMEL RD and VEITH TL (2007) Model evaluation guidelines for systematic quantification of accuracy in watershed simulations. T*rans. ASABE* **50** (3) 885–900. https://doi.org/10.13031/2013.23153
MORILLAS L, LEUNING R, VILLAGARC L and DOMINGO F (2013) Improving evapotranspiration estimates in Mediterranean drylands : the role of soil evaporation. *Water Resour. Res.* **49** 6572–6586. https://doi.org/10.1002/wrcr.20468
MU Q, ZHAO M, and RUNNING SW (2011) Improvements to a MODIS global terrestrial evapotranspiration algorithm. *Remote Sens. Environ.* **115** (8) 1781–1800. https://doi.org/10.1016/j.rse.2011.02.019
MUCINA L, HOARE BD, LTTER MC, DU PREEZ PJ, RUTHERFORD MC, SCOTT-SHAW RC, BREDENKAMP GJ, POWRIE LW, SCOTT L, CAMP KGT, CILLIERS SS, BEZUIDENHOUT H, MOSTERT TH, SIEBERT SJ, WINTER PJD, BURROWS JE, DOBSON L, WARD RA, STALMANS M, OLIVER EGH, SIEBERT F, SCHIMDT E, KOBISI K and KOSE L (2006) The Grassland Biome. In: Mucina L and Rutherford MC (eds) *The Vegetation of South Africa, Lesotho and Swaziland. Strelitzia 19.* South African National Biodiversity Institute, Pretoria.
MYNENI R, ZHANG B, HOFFMAN S, KNYAZIKHIN Y, PRIVETTE JL, GLASSY J, TIAN Y, WANG Y, SONG X, ZHANG Y, SMITH GR, LOTSCH A, FRIEDL M, MORISETTE JT, VOTAVA P, NEMANI RR and RUNNING SW (2002) Global products of vegetation leaf area and fraction absorbed PAR from year one of MODIS data. *Remote Sens. Environ.* **83** (1–2) 214–231. https://doi.org/10.1016/S0034-4257(02)00074-3
NAGLER PL, GLENN EP, NGUYEN U, SCOTT RL and DOODY T (2013) Estimating riparian and agricultural actual evapotranspiration by reference evapotranspiration and MODIS enhanced vegetation index. *Remote Sens.* **5** (8) 3849–3871. https://doi.org/10.3390/rs5083849
PALMER AR, WEIDEMAN C, FINCA A, EVERSON CS, HANAN N and ELLERY W (2014) Modelling annual evapotranspiration in a semi-arid African savanna: functional convergence theory, MODIS LAI and the Penman–Monteith equation. *Afr. J. Range Forage Sci.* **32** (1) 33–39. https://doi.org/10.2989/10220119.2014.931305
PALMER AR and YUNUSA IAM (2011) Biomass production, evapotranspiration and water use efficiency of arid rangelands in the Northern Cape, South Africa. *J. Arid Environ.* **75** (11) 1223–1227. https://doi.org/10.1016/j.jaridenv.2011.05.009
PENMAN HL (1948) Natural evaporation from open water, bare soil, and grass. *Proc. R. Soc. Lond. A. Math. Phys. Sci.* (**A, 194** (S)) 120–145. https://doi.org/10.1098/rspa.1948.0037
PRIESTLEY CHB and TAYLOR RJ (1972) On the assessment of surface heat flux and evaporation using large-scale parameters. *Mon. Weather Rev.* **100** 81–82. https://doi.org/10.1175/1520-0493(1972)100<0081:OTAOSH>2.3.CO;2
RAMBIKUR EH and CHÁVEZ JL (2014) Assessing inter-sensor variability and sensible heat flux derivation accuracy for a large aperture scintillometer. *Sensors* **14** (2) 2150–2170. https://doi.org/10.3390/s140202150
SAVAGE MJ (2009) Estimation of evaporation using a dual-beam surface layer scintillometer and component energy balance measurements. *Agric. For. Meteorol.* **149** 501–517. https://doi.org/10.1016/j.agrformet.2008.09.012
SCHULZE RE (1997) South African atlas of agrohydrology and climatology. WRC Report No. TT82/96. Water Research Commission, Pretoria. ISBN No. 1868452719
SNYMAN HA, INGRAM LJ and KIRKMAN KP (2013) *Themeda triandra:* a keystone grass species. *Afr. J. Range Forage Sci.* **30** (3) 99–125. https://doi.org/10.2989/10220119.2013.831375
STRAHLER AH and MULLER JP (1999) MODIS BRDF albedo product: algorithm theoretical basis document. URL: https://modis.gsfc.nasa.gov/data/atbd/atbd_mod09.pdf (Accessed 31 March 2016).
TARNAVSKY E, GRIMES D, MAIDMENT R, BLACK E, ALLAN R., STRINGER M, CHADWICK R and KAYITAKIRE F (2014) Extension of the TAMSAT satellite-based rainfall monitoring over Africa and from 1983 to present. *J. Appl. Meteorol. Climatol.* **53** (12) 2805–2822. https://doi.org/10.1175/JAMC-D-14-0016.1
TUNICK A (2003) CN2 model to calculate the micrometeorological influences on the refractive index structure parameter. *Environ. Model. Softw.* **18** (2) 165–171. https://doi.org/10.1016/S1364-8152(02)00052-X
WEIDEMAN CI (2013) Linking satellite and point micrometeorological data to estimate vegetation water use: distributed evapotranspiration modelling based on MODIS LAI, Penman-Monteith and functional convergence theory. MSc thesis, Rhodes University.
WILLMOTT JC (1981) On the validation of models. *Phys. Geogr.* **2** (2) 184–194.
ZHANG Y, LEUNING R, HUTLEY LB, BERINGER J, MCHUGH I AN and WALKER JP (2010) Using long - term water balances to parameterize surface conductances and calculate evaporation at

http://dx.doi.org/10.4314/wsa.v44i3.16
Available on website http://www.wrc.org.za
ISSN 1816-7950 (Online) = Water SA Vol. 44 No. 3 July 2018

0.05° spatial resolution. *Water Resour. Res.* **46** 1–14. https://doi.org/10.1029/2009WR008716
ZHANG Y, PEÑA-ARANCIBIA JL, MCVICAR TR, CHIEW FHS, VAZE J, LIU C, LU X, ZHENG H, WANG Y, LIU YY, MIRALLES D and PAN M (2016) Multi-decadal trends in global terrestrial evapotranspiration and its components. *Sci. Rep.* **6** 1–12. https://doi.org/10.1038/srep19124

LIST OF SYMBOLS

Symbol	Definition	Unit	Symbol	Definition	Unit
A_c	Energy flux absorbed by the canopy	MJ·m^{-2}	g_{sx}	Maximum stomatal conductance of leaves at the top of the canopy	m·s^{-1}
A_s	Energy flux absorbed by the soil	MJ·m^{-2}	H	Sensible energy flux	W·m^{-2}
C_n^2	Structure parameter of the refractive index of air	m$^{-2/3}$	h	Canopy height	m
C_p	Specific heat capacity of air	J kg^{-1}·K^{-1}	K_c	Crop coefficient	
d	Zero plane of displacement height	m	L	Distance between the transmitter and the receiver	m
D	Aperture diameter of the scintillometer	m	LAI_{max}	Site-specific long-term maximum leaf area index	m^2·m^{-2}
D_a	Water vapour pressure deficit (VPD) of the air (humidity deficit)	kPa	$LE/\lambda E$	Latent energy flux	W·m^{-2}
e_a	Actual water vapour pressure	kPa	N	Number of samples	
$e_s(T_a)$	Saturation water vapour pressure at air temperature	kPa	R_n	Net radiation	W·m^{-2}
E_S	Soil evaporation	mm	u	Wind speed	m·s^{-1}
ET	Evapotransipiration	mm	U	Mann-Whitney test statistic	
ET_0	Reference evapotranspiration	mm	u_*	Friction velocity	m·s^{-1}
$E_{eq,s}$	Equilibrium soil evaporation	mm	V_x	Wind speed at the height to be extrapolated i.e. canopy height)	m·s^{-1}
$E_{est,i}$	Modelled ET for day i	mm	V_2	Wind speed recorded by the agro-meteorological stations at 2 m from the ground level i.e. (h_2 = 2m)	
$E_{obs,i}$	Observed ET for day i	mm	z	Standard score	
f	Ratio of soil evaporation to the equilibrium rate corresponding to energy absorbed at the soil surface (0–1)		z_{om}	Roughness length governing transfer of momentum	m
F	Function to be minimised		z_{ov}	Roughness length governing transfer of water vapour	m
f_{drying}	Fraction of soil evaporation using the rate of soil drying after precipitation		β	Bowen ratio	
f_{swc}	Fraction of soil evaporation using volumetric soil water content		ε	Slope (s) of the curve relating saturation water vapour pressure to temperature (kPa·K^{-1}) divided by γ	
f_{Zhang}	Fraction of soil evaporation using precipitation and equilibrium evaporation ratio		ρ	Air density	kg·m^{-3}
G	Soil energy flux	W·m^{-2}	θ	Volumetric soil water content	m^3·m^{-3}
G_a	Aerodynamic conductance to water vapour	m·s^{-1}	λ	Scintillometer optical wavelength	nm
G_c	Canopy conductance	m·s^{-1}	α	A parameter controlling the rate of soil drying	day^{-1}
			σ_{lnI}^2	Variance of the natural logarithm of intensity fluctuations	
			γ	Psychrometric constant	kPa·K^{-1}

http://dx.doi.org/10.4314/wsa.v44i3.16
Available on website http://www.wrc.org.za
ISSN 1816-7950 (Online) = Water SA Vol. 44 No. 3 July 2018